

Propagation and Guiding of Intense Laser Pulses in Plasmas

P. Sprangle, E. Esarey, J. Krall, and G. Joyce

Beam Physics Branch, Plasma Physics Division, Naval Research Laboratory, Washington, D.C. 20375-5000

(Received 11 May 1992)

A two-dimensional, axisymmetric, relativistic fluid model describing the propagation of intense laser pulses in plasmas is formulated and numerically evaluated. Relativistic guiding is ineffective in preventing the diffractive spreading of short laser pulses and long pulses become modulated due to relativistic and wake-field effects. Laser pulses can be propagated over many Rayleigh lengths by use of a pre-formed plasma density channel or by tailoring the pulse profile. Ultrahigh axial electric fields can be generated behind the laser pulse.

PACS numbers: 52.40.-w, 52.35.Mw

The propagation of intense laser pulses in underdense plasmas may have widespread importance in a number of areas including laser-plasma acceleration [1-3], x-ray lasers [4], harmonic generation [2,3,5,6], and inertial confinement fusion [7]. The recent development of compact terawatt lasers [8] capable of providing short pulses ($\lesssim 1$ ps) of ultrahigh intensities ($\gtrsim 10^{18}$ W/cm²) and moderate energies ($\gtrsim 10$ J) gives additional impetus to these applications. In vacuum, the focused laser pulse propagation distance is limited to a few Rayleigh lengths, $Z_R = \pi r_{L0}^2/\lambda$, where r_{L0} and λ are the minimum spot size and wavelength of the laser, respectively. In plasmas, nonlinear and relativistic effects associated with intense laser fields can significantly modify the propagation characteristics of the laser [2,3,9-11]. The large ratios between the laser wavelength and other characteristic longitudinal lengths in the system, i.e., laser propagation distance, laser pulse length, and plasma wavelength, make the direct numerical integration of the dynamical equations over extended distances impractical.

In the following, a fully nonlinear, relativistic, two-dimensional axisymmetric laser-plasma propagation model is formulated and numerically evaluated for laser pulses of ultrahigh intensities and arbitrary polarizations. The formulation has a number of unique features which allow for numerical simulations to be carried out over extended laser propagation distances. The appropriate Maxwell fluid equations are recast into a convenient form by (i) performing a change of variables to the speed of light frame, (ii) applying the quasistatic approximation (QSA), (iii) expanding in two small parameters (which are independent of the laser intensity), and (iv) averaging over the short spatial scale length, i.e., the laser wavelength. The resulting equations are here used to study the (i) failure of relativistic focusing for short laser pulses, (ii) modulation of long laser pulses by wake-field effects, (iii) optical guiding of tailored laser pulses, and (iv) use of plasma density channels to guide intense laser pulses.

The plasma is modeled using relativistic cold fluid equations. The momentum and continuity equations are $d\mathbf{u}/dt = c\nabla\phi + \partial\mathbf{a}/\partial t - c\mathbf{u} \times (\nabla \times \mathbf{a})/\gamma$ and $\partial(\rho\gamma)/\partial t + c\nabla \cdot (\rho\mathbf{u}) = 0$, respectively, where $\mathbf{a} = |e|\mathbf{A}/m_0c^2$ and

$\phi = |e|\Phi/m_0c^2$ are the normalized vector and scalar potentials, respectively, $\mathbf{u} = \mathbf{p}/m_0c$ is the normalized fluid momentum, $\rho = n/\gamma n_0$, n is the electron density, n_0 is the ambient density, $\gamma = (1 + \mathbf{u}^2)^{1/2}$ is the relativistic factor, and $-|e|$ and m_0 are the electron charge and rest mass, respectively. The momentum and continuity equations, together with the wave equation and Poisson's equation for \mathbf{a} and ϕ , form a complete description of the laser-plasma interaction. In the following, the Coulomb gauge is used ($\nabla \cdot \mathbf{a} = 0$), the ions are assumed stationary, and thermal effects are neglected [2].

The full set of equations is recast into speed of light coordinates by changing variables from z, t to $\zeta = z - ct$ and $\tau = t$, where z and t are laboratory frame variables denoting the distance along the laser propagation axis and time, respectively. The QSA [2] is then applied. Here, the electron transit time through the laser pulse, which is equal to the laser pulse duration, τ_L , is assumed to be short compared to the laser pulse evolution time, τ_e , which is determined by the pulse diffraction time, $\sim Z_R/c$, or by the pulse dispersion time, $\sim \omega/\omega_p^2$, where ω is the laser frequency and $\omega_p = (4\pi n_0 |e|^2/m_0)^{1/2}$ is the ambient plasma frequency. In the QSA the electrons experience essentially static fields, allowing the $\partial/\partial\tau$ derivatives to be neglected in the fluid equations, but not in the wave equation. The resulting equations are expanded to first order in the parameters $\varepsilon_1 = 1/kr_L \ll 1$ and $\varepsilon_2 = k_p/k \ll 1$, where $k = 2\pi/\lambda$, $k_p = 2\pi/\lambda_p = \omega_p/c$, and r_L is the laser spot size. All the fluid and field quantities are expanded in slow and fast terms, i.e., $\mathbf{Q} = \mathbf{Q}_s + \mathbf{Q}_f$. The fast quantities are of the general form $\mathbf{Q}_f = \frac{1}{2}\hat{\mathbf{Q}}_f(r, \zeta, \tau) \times \exp(imk\zeta) + \text{c.c.}$, where $m = 1, 2, 3, \dots$ and $\hat{\mathbf{Q}}_f$ is complex and slowly varying in ζ . Within this representation, the nonlinear fluid equations are averaged over the laser wavelength in the (ζ, τ) frame. The ζ averaging allows for all the laser-plasma response quantities to be evaluated on the slow spatial scale, i.e., λ_p or $c\tau_L$, permitting solutions over extended propagation distances.

The resulting equations describe the slowly varying components of the fluid and field quantities:

$$\nabla_{\perp}^2 \mathbf{a} = k_p^2 \rho \mathbf{u} - \partial(\nabla\phi)/\partial\zeta, \quad (1a)$$

$$\nabla_{\perp}^2 \phi + \partial^2 \phi / \partial \zeta^2 = k_p^2 (\gamma \rho - \rho^{(0)}), \quad (1b)$$

$$\partial(\mathbf{u} - \mathbf{a})/\partial\zeta = \nabla(\gamma - \phi), \quad (1c)$$

$$\partial[\rho(1 + \psi)]/\partial\zeta = \nabla_{\perp} \cdot (\rho \mathbf{u}_{\perp}), \quad (1d)$$

where the subscript s , denoting the slow component of the quantity, has been dropped, $\rho^{(0)} = n^{(0)}/n_0$, $n^{(0)}(r)$ is the initial plasma density profile prior to the laser interaction which may be a function of radial position, and $\psi = \phi - a_z$ is the wake potential. Equations (1a)–(1d) represent, respectively, the slow components of the wave, Poisson's, momentum, and continuity equations.

In obtaining Eq. (1c), the identity $\nabla \times (\mathbf{u} - \mathbf{a}) = 0$, showing the irrotational nature of the ponderomotive flow, was used. It can be shown that the quantity $\gamma - u_z - \psi$ is an invariant which is set equal to unity, i.e., its value prior to the arrival of the laser pulse. The slowly varying component of the relativistic factor is

$$\gamma = (1 + \psi)^{-1} [1 + \mathbf{u}_{\perp}^2 + |\hat{\mathbf{a}}_f|^2/2 + (1 + \psi)^2]/2, \quad (2)$$

where a linearly polarized laser pulse with amplitude $|\hat{\mathbf{a}}_f|$ is assumed throughout this paper. The transverse component of the laser radiation field is $\mathbf{a}_f = \hat{\mathbf{a}}_f(r, \zeta, \tau) \times \exp(ik\zeta)/2 + \text{c.c.}$, where $\hat{\mathbf{a}}_f$ is the complex, slowly varying amplitude which satisfies the parabolic (reduced) wave equation,

$$(\nabla_{\perp}^2 + 2c^{-1}k \partial/\partial\tau) \hat{\mathbf{a}}_f = k_p^2 \rho \hat{\mathbf{a}}_f. \quad (3)$$

Within the QSA, the self-consistent, slowly varying equations in the (ζ, τ) variables, describing the laser-plasma interaction, to first order in ε_1 and ε_2 , are given by Eqs. (1)–(3).

Equations (1a)–(1d) can be combined to yield a single equation for ψ in terms of $|\hat{\mathbf{a}}_f|^2$ of the form $\partial^2\psi/\partial\zeta^2 = G(\psi, |\hat{\mathbf{a}}_f|^2)$, where G is an involved function. The equation for ψ is obtained by noting that $\rho = (\rho^{(0)})$

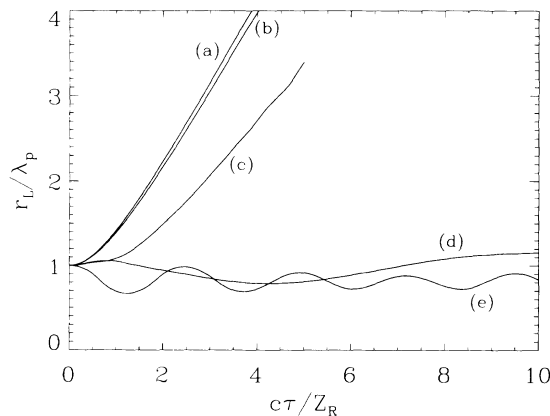


FIG. 1. Laser spot size r_L (at $\zeta = -L/2$) vs propagation distance normalized to the Rayleigh length, $c\tau/Z_R$, for (a) vacuum diffraction, (b) an ultrashort pulse with $L = \lambda_p/4$, (c) a short pulse with $L = \lambda_p$, (d) a shaped pulse, and (e) a channel-guided pulse. The spot size is normalized to the plasma wavelength $\lambda_p = 0.03$ cm.

$+k_p^{-2}\nabla_{\perp}^2\psi)/(1 + \psi)$ and $\mathbf{u}_{\perp} = \rho^{-1}k_p^{-2}\nabla_{\perp}\partial\psi/\partial\zeta$. Note also that the refractive index is solely a function of ψ through ρ , i.e., $\eta_R = 1 - k_p^2\rho/2k^2$. Equation (3) together with $\partial^2\psi/\partial\zeta^2 = G$ completely describe the 2D-axisymmetric laser-plasma interaction. The wake potential ψ is related to the axial electric field E_z of plasma response (wake field) by $\hat{E}_z = -\partial\psi/\partial\zeta$, where $\hat{E}_z = |e|E_z/m_0c^2$.

Equations (1)–(3) reduce to models which have been previously studied, i.e., the broad pulse limit ($\nabla_{\perp} \rightarrow 0$) [2] and the axially uniform pulse limit ($\partial/\partial\zeta \rightarrow 0$) [10]. Reference [2] showed theoretically that relativistic guiding, which requires laser powers (in units of GW) $P \geq P_{\text{crit}} = 17(\lambda_p/\lambda)^2$, does not occur for short pulses, $c\tau_L < \lambda_p/(1 + |\hat{\mathbf{a}}_f|^2/2)^{1/2}$. For short pulses the plasma cannot collectively respond to modify the refractive index.

Simulations of short pulse propagation confirm the predictions of Ref. [2]. The results are shown in Fig. 1 for the parameters $\lambda_p = 0.03$ cm ($n_0 = 1.2 \times 10^{16}$ cm $^{-3}$), $r_L = \lambda_p$ (Gaussian radial profile), $\lambda = 1$ μm ($Z_R = 28$ cm), and $P = P_{\text{crit}}$. The initial axial laser profile is given by $|\hat{\mathbf{a}}_f(\zeta)| = a_0 \sin(-\pi\zeta/L)$ for $0 < -\zeta < L = c\tau_L$, where $a_0 = 0.9$ for the above parameters. Simulations are performed for two laser pulse lengths, $L = \lambda_p$ ($\tau_L = 1$ ps) and $L = \lambda_p/4$ ($\tau_L = 0.25$ ps). The initial normalized laser intensity, $|\hat{\mathbf{a}}_f|^2$, is shown in Fig. 2 for $L = \lambda_p$. The spot size at the pulse center versus propagation distance $c\tau$ is shown in Fig. 1 for (a) the vacuum diffraction case, (b) the $L = \lambda_p/4$ pulse, and (c) the $L = \lambda_p$ pulse. The $L = \lambda_p/4$ pulse diffracts almost as if in vacuum. The $L = \lambda_p$ pulse experiences a small amount of initial guiding before diffracting.

The wake field generated by the finite rise time of a long pulse can modulate the pulse structure. Consider a long laser pulse in which the body of the pulse has a constant amplitude with $P = P_{\text{crit}}$ and, therefore, should be relativistically guided. The amplitude of the wake field generated by the front of the pulse is determined by the

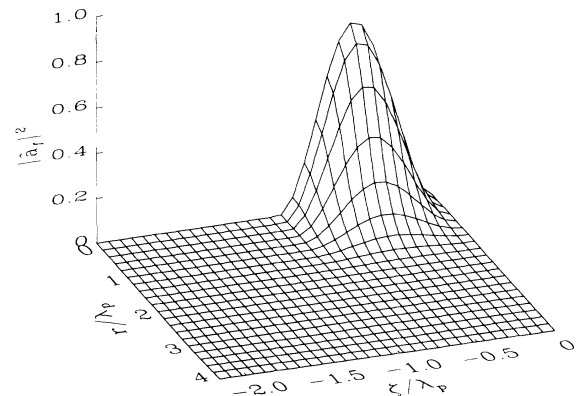


FIG. 2. Normalized laser intensity $|\hat{\mathbf{a}}_f|^2$ in the speed of light frame (ζ, τ) at $\tau = 0$ for the parameters $a_0 = 0.9$, $L = r_L = \lambda_p = 0.03$ cm, and $\lambda = 1$ μm . In the (ζ, τ) frame, the plasma flows from right to left.

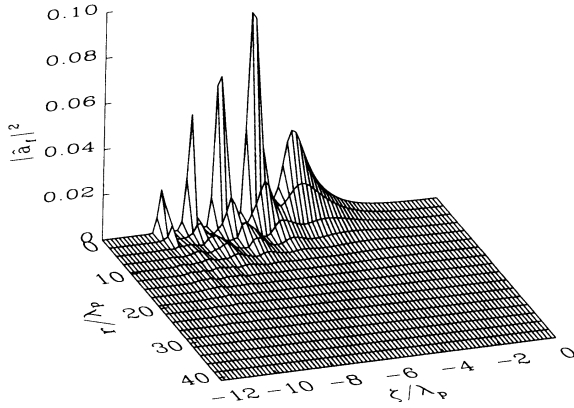


FIG. 3. Normalized laser intensity $|\hat{a}_f|^2$ at $c\tau = 2Z_R$ for a long pulse showing modulation.

rise time. The wake field, which consists of a plasma density modulation of the form $\delta n = \delta n_0(r)\cos(k_p\zeta)$, modifies the plasma's refractive index [11]. In regions of a local density channel, i.e., where $\partial\delta n/\partial r > 0$, the radiation focuses. In regions where $\partial\delta n/\partial r < 0$, diffraction is enhanced.

Pulse modulation is illustrated by a simulation of a long pulse (a long rise, $L_{\text{rise}} = 5\lambda_p$, followed by a long flattop region, $L_{\text{flat}} = 5\lambda_p$) with $P = P_{\text{crit}}$ ($a_0 = 0.09$, $r_L = 10\lambda_p$, $\lambda_p = 0.03$ cm, and $\lambda = 1$ μm). Simulations indicate that for $P \geq P_{\text{crit}}$, an unstable wake field is excited at the front of the pulse and rapidly modulates the pulse profile. Figure 3 shows the pulse modulation, where $|\hat{a}_f|^2$ is plotted at $c\tau = 2Z_R$ for the above initial parameters.

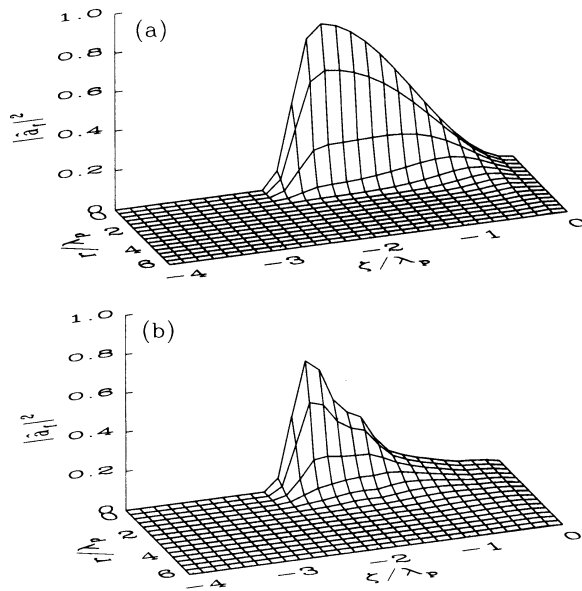


FIG. 4. Normalized laser intensity $|\hat{a}_f|^2$ at (a) $\tau = 0$ and at (b) $c\tau = 24Z_R$ for a tailored pulse.

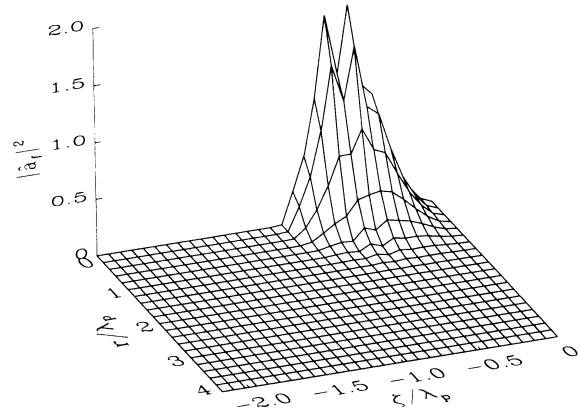


FIG. 5. Normalized laser intensity $|\hat{a}_f|^2$ at $c\tau = 10Z_R$ for the laser pulse of Fig. 2 propagating in a plasma density channel.

At high intensities, i.e., $a_0^2 \gg 1$, the modulation is reduced.

A tailored laser pulse can propagate many Rayleigh lengths without significantly altering its original profile. Consider a long laser pulse, $c\tau_L \gg \lambda_p$, in which the spot size is tapered from a large value at the front to a small value at the back, so that the laser power, $P \sim r_L^2 |\hat{a}_f|^2$, is consistent throughout the pulse and equal to P_{crit} . The leading portion ($\ll \lambda_p$) of the pulse will diffract as if in vacuum [2]. However, since r_L is large at the front of the pulse, the Rayleigh length is also large. Hence, the locally large spot size allows the pulse front to propagate a long distance, whereas the body of the pulse will be relativistically guided. Also, since $|\hat{a}_f|^2$ increases slowly throughout the pulse, detrimental wake-field effects are reduced.

Figure 4(a) shows the initial profile of a tailored pulse in which $|\hat{a}_f|$ increases from 0.09 to 0.9 over a length $L_{\text{rise}} = 2\lambda_p$. Here, $P = P_{\text{crit}}$ throughout the pulse, $|\hat{a}_f| r_L = 0.9\lambda_p$ ($\lambda_p = 0.03$ cm, $\lambda = 1$ μm), which implies a de-

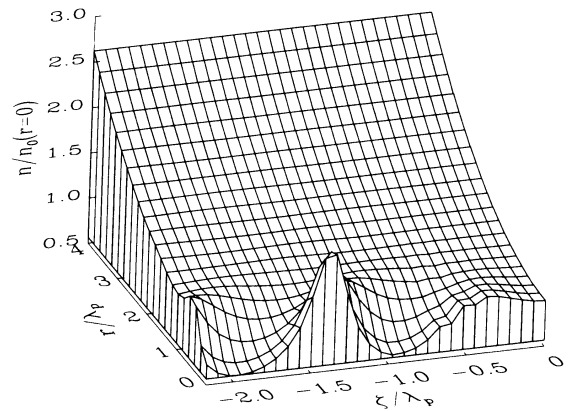


FIG. 6. Plasma electron density n/n_0 at $c\tau = 10Z_R$ for the channel-guided case.

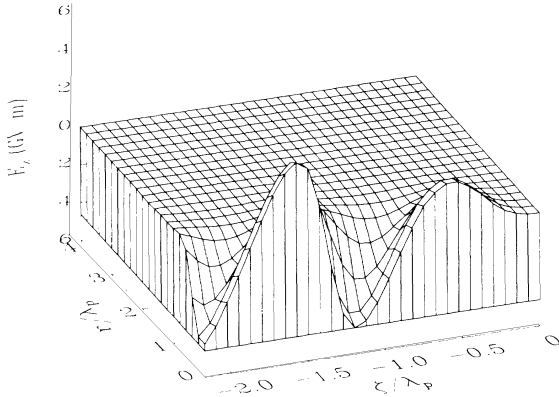


FIG. 7. Axial electric field E_z at $c\tau = 10Z_R$ for the channel-guided case.

crease in r_L from $10\lambda_p$ to λ_p . At peak intensity the vacuum diffraction length is $Z_R = 28$ cm. The effectiveness of pulse tailoring can be seen by the $r_L(c\tau)$ plot in Fig. 2(d) and in Fig. 4(b), where a plot of $|\hat{a}_f|^2$ at $c\tau = 24Z_R$ demonstrates that the pulse is distorted but largely intact. At $c\tau = 24Z_R = 6.8$ m, the peak axial electric field of the wake field behind the pulse is $E_z = 1.3$ GeV/m.

A preformed plasma density channel can guide short, intense laser pulses. In the weak laser pulse limit, $|\hat{a}_f|^2 \ll 1$, the index of refraction is given by $n_R = 1 - k_p^2 \rho^{(0)}/2k^2$. Optical guiding requires $\partial n_R / \partial r < 0$, hence, a preformed density channel, $n^{(0)}(r) = n_0 \rho^{(0)}(r)$, may prevent pulse diffraction. Analysis of the wave equation in the weak pulse limit indicates that a parabolic density channel will guide a Gaussian laser beam provided that the depth of the density channel [3] is $\Delta n = 1/\pi r_e r_L^2$, where $\Delta n = n^{(0)}(r_L) - n^{(0)}(0)$ and r_e is the classical electron radius.

A simulation of channel guiding is shown in Figs. 5–7 for a laser pulse with the initial conditions of Fig. 2 propagating in a parabolic density channel with $\Delta n = 1.3 \times 10^{15} \text{ cm}^{-3}$ and $n^{(0)}(0) = 1.2 \times 10^{16} \text{ cm}^{-3}$. Figure 5 shows the laser intensity at $c\tau = 10Z_R$. The laser pulse shows some distortions but remains essentially guided. Guiding is confirmed by the $r_L(c\tau)$ plot in Fig. 2(e). The $r_L(c\tau)$ oscillations indicate a slight mismatch between the laser and channel parameters. This is caused by the laser pulse further reducing the density in the region of peak intensity as can be seen in Fig. 6. The axial wake field E_z , plotted in Fig. 7, shows a peak amplitude of 4.6 GeV/m. Additional simulations have shown that the

large wake fields generated by a guided pulse can longitudinally and transversely trap and accelerate a trailing electron bunch to high energies.

This work was supported by the Department of Energy and the Office of Naval Research.

-
- [1] T. Tajima and J. M. Dawson, Phys. Rev. Lett. **43**, 267 (1979); L. M. Gorbunov and V. I. Kirsanov, Zh. Eksp. Teor. Fiz. **93**, 509 (1987) [Sov. Phys. JETP **66**, 290 (1987)]; P. Sprangle, E. Esarey, A. Ting, and G. Joyce, Appl. Phys. Lett. **53**, 2146 (1988); E. Esarey, A. Ting, P. Sprangle, and G. Joyce, Comments Plasma Phys. Controlled Fusion **12**, 191 (1989).
 - [2] P. Sprangle, E. Esarey, and A. Ting, Phys. Rev. Lett. **64**, 2011 (1990); Phys. Rev. A **41**, 4463 (1990); A. Ting, E. Esarey, and P. Sprangle, Phys. Fluids B **2**, 1390 (1990).
 - [3] P. Sprangle and E. Esarey, Phys. Fluids B (to be published).
 - [4] J. C. Solem, T. S. Luk, K. Boyer, and C. K. Rhodes, IEEE J. Quantum Electron. **25**, 2423 (1989).
 - [5] F. Brunel, J. Opt. Soc. Am. B **7**, 521 (1990); E. Esarey, G. Joyce, and P. Sprangle, Phys. Rev. A **44**, 3908 (1991); W. Mori, Phys. Rev. A **44**, 5118 (1991).
 - [6] P. Sprangle and E. Esarey, Phys. Rev. Lett. **67**, 2021 (1991); E. Esarey and P. Sprangle, Phys. Rev. A **45**, 5872 (1992).
 - [7] G. Mourou and D. Umstadter, Phys. Fluids B (to be published); X. Liu and D. Umstadter, Phys. Rev. Lett. **69**, 1935 (1992).
 - [8] D. Strickland and G. Mourou, Opt. Commun. **56**, 216 (1985); P. Maine, D. Strickland, P. Bado, M. Pessot, and G. Mourou, IEEE J. Quantum Electron. **24**, 398 (1988); M. D. Perry, F. G. Patterson, and J. Weston, Opt. Lett. **15**, 1400 (1990).
 - [9] A. G. Litvak, Zh. Eksp. Teor. Fiz. **57**, 629 (1969) [Sov. Phys. JETP **30**, 344 (1970)]; C. Max, J. Arons, and A. B. Langdon, Phys. Rev. Lett. **33**, 209 (1974); P. Sprangle, C. M. Tang, and E. Esarey, IEEE Trans. Plasma Sci. **15**, 145 (1987); E. Esarey, A. Ting, and P. Sprangle, Appl. Phys. Lett. **53**, 1266 (1988); W. B. Mori, C. Joshi, J. M. Dawson, D. W. Forslund, and I. M. Kindel, Phys. Rev. Lett. **60**, 1298 (1988).
 - [10] G. Z. Sun, E. Ott, Y. C. Lee, and P. Guzdar, Phys. Fluids **30**, 526 (1987); T. Kurki-Suonio, P. J. Morrison, and T. Tajima, Phys. Rev. A **40**, 3230 (1989); P. Sprangle, A. Zigler, and E. Esarey, Appl. Phys. Lett. **58**, 346 (1991); A. B. Borisov, A. V. Borovskiy, O. B. Shiryayev, V. V. Korobkin, A. M. Prokhorov, J. C. Solem, T. S. Luk, K. Boyer, and C. K. Rhodes, Phys. Rev. A **45**, 5830 (1992).
 - [11] E. Esarey and A. Ting, Phys. Rev. Lett. **65**, 1961 (1990).